Ab initio calculations of elastic and magnetic properties of Fe, Co, Ni, and Cr crystals under isotropic deformation

M. Černý,[1] J. Pokluda,[1] M. Šob,[2,*] M. Friák,[2] P. Šandera[1]
[1]*Institute of Engineering Physics, Faculty of Mechanical Engineering, Brno University of Technology, Technická 2, CZ–616 69 Brno, Czech Republic*
[2]*Institute of Physics of Materials, Academy of Sciences of the Czech Republic, Žižkova 22, CZ–616 62 Brno, Czech Republic*
(Received 13 June 2002; published 30 January 2003)

Ab initio electronic structure calculations of the ideal strength of Fe, Co, Ni, and Cr under isotropic tension were performed using the linear muffin-tin orbital method in the atomic sphere approximation. Magnetic ordering was taken into account by means of a spin-polarized calculation. Two approximations for the exchange-correlation term were employed: namely, the local (spin) density approximation and the generalized gradient approximation. Computed values of equilibrium lattice parameters, bulk moduli, and magnetic moments were compared with available experimental data. The stability of the ground-state structure in the tensile region was assessed via comparison of its total energy and enthalpy with those of some other structures. No instabilities were found before reaching the inflection point on the total energy versus volume curve and the stress related to this point was therefore considered to be the ideal strength.

DOI: 10.1103/PhysRevB.67.035116 PACS number(s): 61.50.Ah, 61.66.Bi, 71.15.Mb, 75.50.Bb

I. INTRODUCTION

Triaxial tension occurs in solids in the vicinity of some types of defects in the microstructure of crystalline solids, e.g., cracks, pores, voids, and complex phase or grain boundaries.[1] Very often, bonds are broken in the region of a defect which means that the corresponding stresses approach the level of the maximum stress which can be accommodated by the material, i.e., the theoretical (ideal) strength. To understand the structure and behavior of these defects, information on local elastic constants and ideal strength is necessary. For example, knowledge of the ideal strength at triaxial tension σ_{id} and the ideal shear strength allows for assessment of both the ductile-brittle response and the crack stability in solids.[2]

Most calculations of σ_{id} have been based on semiempirical potentials with the parameters adjusted to the experimental data near the equilibrium state.[3] However, the σ_{id} value is usually associated with the inflection point on the total energy versus volume curve, which is far from equilibrium. During the last years, several *ab initio* methods were used for σ_{id} calculations for number of cubic metals[4–6] without magnetic order. Song, Yang, and Li[6] computed the electronic structure and related elastic properties by means of the discrete variational cluster method. Nevertheless, this method significantly underestimates values of the equilibrium lattice parameter.

For any realistic *ab initio* calculation of the deformation behavior of crystals exhibiting magnetic ordering as ferromagnetism or antiferromagnetism, spin polarization must be properly taken into account. Many authors, e.g., Refs. 7–12, have shown that neglect of magnetic ordering leads to wrong ground-state structure properties of Fe, Co, and Ni. A prevalent number of *ab initio* studies of magnetic crystals concerned their behavior near the minimum of the total energy versus crystal volume curve.

Recently, some *ab initio* analyses of different uniaxial deformation paths in Fe or Co far away from the energy minimum were performed.[13–16] Calculated phase boundaries can be used, e.g., to predict the lattice parameters and magnetic states of iron overlayers on metallic substrates.[17] Moreover, Söderlind *et al.*[18] have published an extended study of the Fe phase diagram in the compressive hydrostatic stress region including elastic properties. Krasko and Olson[19] also investigated the energetics of iron predominantly under hydrostatic compression. In all those calculations, both nonmagnetic (non-spin-polarized) and the magnetic (spin-polarized with ferromagnetic ordering) treatments have been employed.

The main purpose of this paper is to compute the mechanical and magnetic characteristics of Fe, Co, Ni, and Cr crystals under isotropic (triaxial) tensile deformation using *ab initio* approaches with and without spin polarization. The reliability of individual approaches can be assessed by comparison of the computed values of the equilibrium lattice constant, bulk modulus, and magnetic moment with experimental data. Special attention is paid to the maximum attainable stress and a comparison of the energy and enthalpy of some possible competing structures, providing a simple test of the ground-state structure stability.

II. DETAILS OF THE CALCULATIONS

The equilibrium lattice constant a_0, bulk modulus B, and maximum stress σ_{max} were calculated from the dependence of the total energy per atom, E_{tot}, on the atomic volume V. The applied stress σ at any V can be determined according to the relation[4]

$$\sigma = \frac{dE_{tot}}{dV}.$$

Here we consider a quasireversible deformation process at zero absolute temperature. The stress approaches its maximum σ_{max} at the point of inflection provided that there are

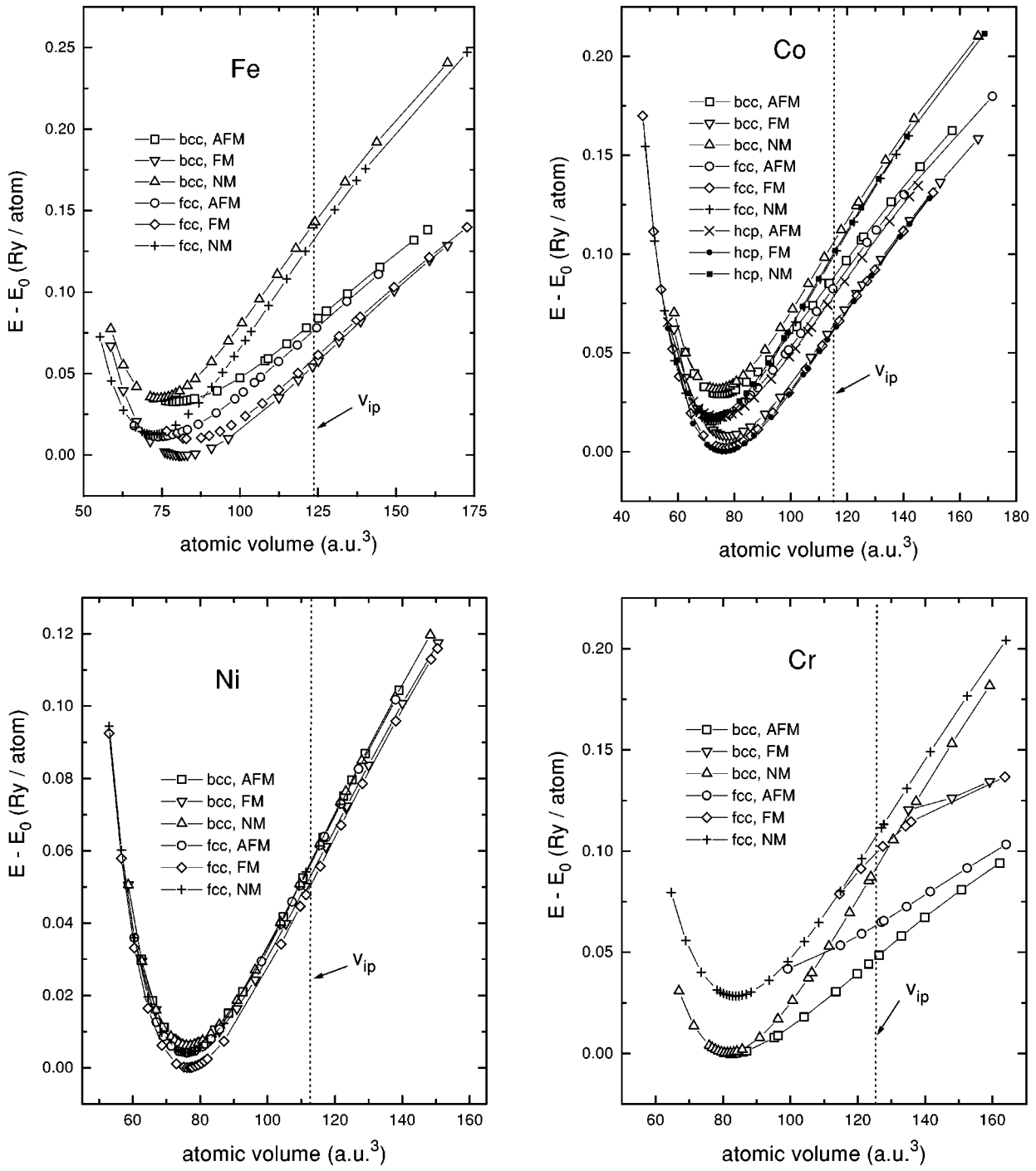

FIG. 1. Total energy as a function of atomic volume. The dotted line represents the volume V_{ip} related to the inflection point on the ground-state structure energy profile.

no other structure instabilities at lower stresses. The bulk modulus may be obtained from

$$B = V \left. \frac{d^2 E_{tot}}{dV^2} \right|_{V=V_0},$$

where V_0 is the atomic volume in the undeformed state. The enthalpy per atom can be determined using the relation

$$H = E_{tot} - \sigma V.$$

For the total energy evaluation, the linear muffin-tin orbital method in the framework of the atomic sphere approximation (LMTO-ASA) was applied.[20,21] This method is particularly suitable for closely packed structures like fcc or bcc or for comparing the energies of atomic configurations with the same symmetry.[21,22] Moreover, it represents one of the fastest *ab initio* approaches in such cases. The main approxi-

TABLE I. Total energy minima (mRy/atom) with respect to the ground-state energy minima in Fe, Co, Ni, and Cr (GGA results).

Metal	NM			(A)FM		
	bcc	fcc	hcp	bcc	fcc	hcp
Fe	34.7	12.6	-	0	10.1	-
Co	31.4	15.4	17.6	8.0	1.9	0
Ni	6.1	4.2	-	5.2	0	-
Cr	0.3	28.4	-	0 [a]	28.4 [a]	-

[a]The AFM result.

mations used in the LMTO-ASA method are as follows: (i) the Wigner-Seitz cell is approximated by a sphere, and (ii) the potential and total energies are calculated from spherically averaged charge densities. Due to these approximations, the LMTO-ASA method is not suitable for comparison of the total energies of systems with different symmetry. The reason for this is the above-mentioned geometry violation in the ASA and an error in the calculation of the electrostatic term in the total energy.[23] In the case of systems with the same symmetry, the sum of errors due to the geometry violation and electrostatic term is roughly the same and, therefore, the total energy differences may be considered as quite reliable.

In our calculations, the basis consisted of LMTO's of *s*, *p*, and *d* symmetry and *f* orbitals were downfolded. The combined-correction term[21,22] was included. This approach gives probably the best performance the LMTO-ASA method may provide.[22,24] The exchange-correlation energy was evaluated using both the local (spin) density approximation[25] (LDA) and the generalized gradient approximation[26] (GGA).

The scalar-relativistic approach was applied to include relativistic effects. The number of **k** points in the whole Brillouin zone has been set to 4096 (16×16×16).

III. COMPUTED RESULTS AND DISCUSSION

A. Variations of the total energy and magnetic moment under triaxial deformation

The $E_{tot}(V)$ profiles obtained from both non-spin-polarized [nonmagnetic (NM)] and spin-polarized calculations with ferromagnetic (FM) or antiferromagnetic (AFM) ordering (only collinear magnetism is considered for all cases and the CsCl structure is adopted for AFM ordering) are shown for all metals investigated in Fig. 1. These curves were obtained using the GGA since the LDA yields a wrong ground state for Fe (see, e.g., Ref. 9). Moruzzi and Marcus[27,28] have shown that in some 3*d* or 4*d* transition metals the AFM states can exhibit a lower total energy than the FM or NM states at large volumes. However, it is not the case of Fe, Co, and Ni (Fig. 1).

Computed values of the differences between the total energy minimum of the ground-state structure and the minima of the other considered structures obtained by means of the GGA are displayed in Table I for all investigated metals. It may be seen that the experimentally observed ground-state

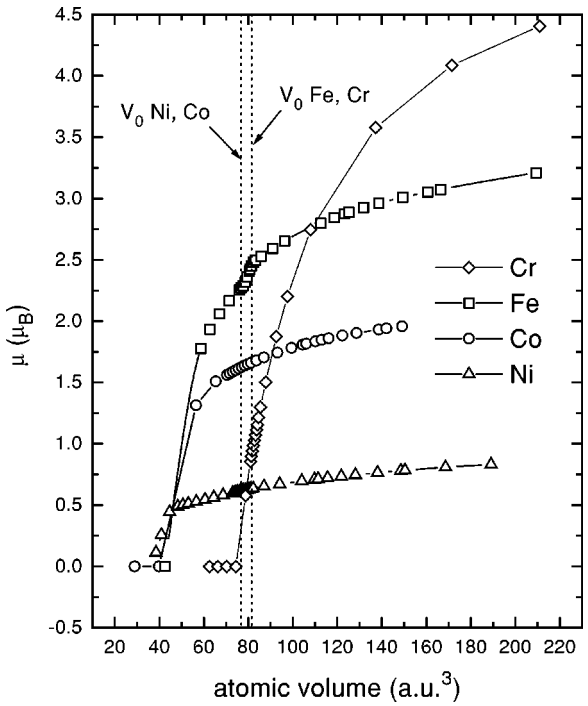

FIG. 2. Magnetic moment μ per atom as a function of atomic volume. The dotted lines represent equilibrium atomic volumes V_0. Note that the V_0 of Co and Ni are almost identical as well as are those of Fe and Cr (see Fig. 1).

structures are correctly reproduced. The energy difference between the NM and (A)FM minima is usually called the magnetic energy. In the case of Fe bcc structure, our value of 34.7 mRy/atom is well comparable with the values of 35.1 mRy/atom and 38.0 mRy/atom reported in Refs. 12 and 29. The value of 21 mRy/atom obtained by the Korringa-Kohn-Rostoker[30] (KKR) method is in a good agreement with our LDA result (16.7 mRy/atom) due to the same approximation of the exchange-correlation term.

The calculated ground-state structure of cobalt is FM hcp (Fig. 1). The total energies of bcc and fcc structures with FM ordering are a little bit higher than the hcp one. However, they remain higher in the whole computed region of tensile stress. In our calculations, the experimental c/a ratio value[31] of 1.6215 was kept constant for all volumes. Again, the magnetic energy obtained using the LDA (6.8 mRy/atom) corresponds well to the value of 8.1 mRy/atom reported in Ref. 30. However, the GGA result is higher (see Table I).

In case of the Ni fcc structure, the magnetic energy is much smaller than that for Fe. It lies between the values of 6.2 mRy/atom and 2.6 mRy/atom reported in Refs. 10 and 29, respectively.

The lowest magnetic energy of 0.3 mRy/atom (the difference between the NM and AFM energy minimum) found in case of Cr bcc structure (Fig. 1) is significantly lower than the result of 1.18 mRy/atom obtained by Guo and Wang.[32] On the other hand, the energy difference between the fcc and bcc structures of 28.1 mRy/atom published by those authors matches our value of 28.4 mRy/atom quite well. The $E_{tot}(V)$ dependences in Fig. 1 for the bcc structure look qualitatively similar to those published in Ref. 27, where the augmented

TABLE II. Ground-state structure characteristics and theoretical strengths calculated within the GGA and LDA. Here a_0 is the equilibrium lattice parameter, B is the bulk modulus, μ is the magnetic moment per atom, σ_{max} is the stress at the inflection point, and a_{ip} is the corresponding lattice parameter. The μ values are calculated at the corresponding computed a_0.

Element	Property	LDA NM	GGA NM	LDA (A)FM	GGA (A)FM	Experiment
	a_0 (a.u.)	5.12	5.29	5.22	5.47	5.41 [a]
	B (GPa)	332	257	260	129	168 [b]
	μ (μ_B)			2.04	2.47	2.22 [a]
Fe	σ_{max} (GPa)	52.4	39.5	37.7	26.7	
bcc	a_{ip}/a_0	1.15	1.15	1.16	1.15	
	c_0 (a.u.)	7.34	7.61	7.44	7.74	7.69 [a]
	B (GPa)	323	239	288	181	191 [b]
	μ (μ_B)			1.50	1.62	1.72 [a]
Co	σ_{max} (GPa)	49.6	36.1	43.1	30.7	
hcp	a_{ip}/a_0	1.14	1.15	1.15	1.15	
	a_0 (a.u.)	6.46	6.72	6.47	6.74	6.65 [a]
	B (GPa)	270	192	269	186	186 [b]
	μ (μ_B)			0.56	0.61	0.60 [a]
Ni	σ_{max} (GPa)	40.2	28.0	39.5	27.4	
fcc	a_{ip}/a_0	1.14	1.14	1.14	1.14	
	a_0 (a.u.)	5.30	5.46	5.30	5.49	5.44 [a]
	B (GPa)	288	241	301	185	190 [b]
Cr	σ_{max} (GPa)	51.2	41.1	37.2	21.0	
bcc	a_{ip}/a_0	1.16	1.16	1.11	1.14	

[a]Reference 35.
[b]Reference 31.

spherical waves method and LSDA were used. The only, but important, difference is the fact that the ground-state structure found in Ref. 27 is nonmagnetic. Our calculations predict the AFM bcc structure to be the ground-state structure in accordance with Ref. 32 and experimental findings.

The dependence of magnetic moment versus volume, $\mu(V)$, for Fe, Co, Ni, and Cr in their ground-state structures is plotted in Fig. 2. The dotted lines correspond to the equilibrium volumes V_0 of all metals displayed. The magnetic moment decreases with a decreasing volume and vanishes when the volume V approaches $0.5V_0$. These findings are in accordance with results published previously.[33,34] The only exception is the case of Cr, where μ vanishes at a volume slightly smaller than the equilibrium one. It should result in a strong $\mu(V)$ dependence of chromium in the unstressed state. This finding is supported also by the previous work of Moruzzi and Marcus.[27]

An interesting feature seems to be the local wavy behavior of the magnetic moment of iron near the equilibrium volume. It predicts a high sensitivity of the μ with respect to volume changes near the equilibrium. The existence of this phenomenon can be indicated also from the results of Moroni *et al.*[33] However, it could not be clearly declared by those authors due to an insufficient number of computed points in the vicinity of V_0. With increasing volume, μ is expected to increase monotonously to a saturation value which is equal to the value of the magnetic moment of a free atom (obeying the Hund rule).

B. Crystal properties in the ground state

Computed values of the equilibrium lattice constant a_0, bulk modulus B, and magnetic moment μ are shown in Table II and compared with experimental data.[31,35]

Our LDA NM result of $B=332$ GPa for iron is in good agreement with the value of 306 GPa published by Moruzzi, Janak, and Williams[30] for the non-spin-polarized calculation. By using the spin-polarized calculation, they obtained a value in better accordance with experiment. As can be seen from Table II, our LMTO results exhibit similar trends. The value of the magnetic moment $\mu=2.47\mu_B$ was obtained for the computed $a_0=5.47$ a.u. When using the experimental lattice parameter, the corresponding calculated value $\mu=2.34\mu_B$ is in better agreement with the experimental one and also with the value of $2.32\mu_B$ published in Ref. 36.

A comparison of computed and experimental values for the Co hcp structure shows that the FM GGA calculation yields the most satisfactory results. The magnetic moment values at the computed a_0 match the results of $1.50\mu_B$ and $1.63\mu_B$ obtained previously by means of the linear combination of atomic orbitals (LCAO) method[9] employing the LDA and GGA, respectively.

Inclusion of the spin polarization has only a very small effect on all computed values for Ni since both the FM and NM curves are almost identical. Our LDA calculations match well the results obtained by Moruzzi *et al.*[30] On the other hand, the employment of the GGA gives remarkably better agreement with the experiment than does the LDA.

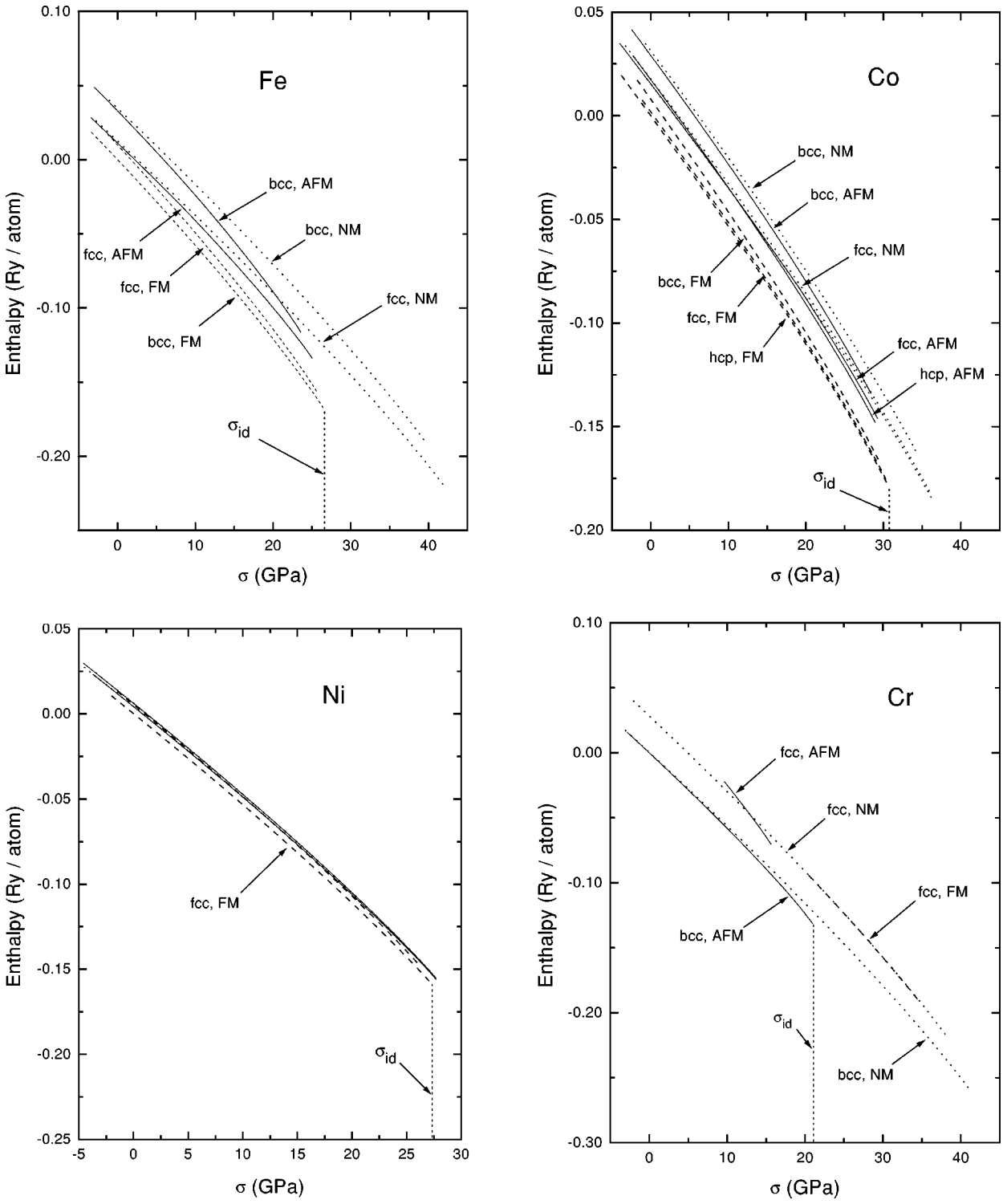

FIG. 3. Enthalpy per atom as a function of applied triaxial stress. The solid, dashed, and dotted lines represent the enthalpies of the AFM, FM, and NM states, respectively. In the case of Ni, the curves other than the ground-state one are almost identical.

Our calculations do not reveal the existence of the FM state in the bcc Cr below the atomic volume of about 135 a.u.[3] The lowering of E_{tot} of the bcc NM state by the onset of the FM state occurs at large volumes, in the instability region after reaching the inflection point (see Fig. 1). The $E_{tot}(V)$ curve for the NM bcc state is substantially steeper than that for the AFM bcc state. The value of $B=241$ GPa for the NM bcc state calculated within the GGA is somewhat higher than the experimental value and than the result computed for the bcc AFM state. The values of $a_0=5.30$ a.u. and $B=270$ GPa reported in Ref. 30 correspond to those obtained by means of our LDA NM calculation, owing to the same applied approximations. On the other hand, using the AFM ordering of spins together with GGA results in a curve

which is much more shallow in the tension area and yields the largest a_0 and the lowest B values in the best agreement with experimental data. The computed magnetic moment at equilibrium volume (here, the atomic moment in AFM ordering) of $1.03\mu_B$ agrees well with previous calculations.[27,32]

C. Phase stability and ideal strength

As was shown in the previous section, GGA spin-polaized calculations slightly overestimate a_0 while underestimating B when compared with the experiment. In spite of this fact, it leads to the best agreement with experiment in most cases. Thus, one can expect that this method will also provide the most reliable values of stress.

The values of the computed maximum stress σ_{max} at the inflection point and of the relative linear extension a_{ip}/a_0 (with a_{ip} being the lattice constant at the inflection point) are shown in Table II. The ideal strength of the material at triaxial extension is related to the inflection point on the dependence of total energy versus volume if some other instability does not occur before this point is reached. In this case, the stress σ_{max} is the maximum stress the material can accommodate.

Breaking the stability condition is usually accompanied by the possibility to change the crystal structure. As a simple test of stability, one could compare the total energies of various crystal structures at the corresponding atomic volume. As can be seen from Fig. 1, the ground-state structure remains energetically more favorable than the other investigated structures until the inflection point is reached (at the volume V_{ip}).

Similarly, one can compare the energetics of metals investigated in terms of enthalpy as a function of stress (negative pressure).[19,37] The enthalpy curves shown in Fig. 3 were obtained by means of a cubic spline based on the GGA data. Again, it is evident that the correct ground-state structure has the lowest enthalpy in the whole region of tensile stresses. Thus, there is no suggestion of any instability before reaching the point of inflection and the related σ_{max} values can be considered to be the ideal strengths σ_{id} of crystals. At present, the corresponding experimental σ_{id} data do not exist owing to the enormous technical problems associated with the application of the isotropic tension to whiskers.

In the region of tensile stresses, the enthalpy profiles in Fig. 3 are plotted only up to the points where the negative pressures become maximum ($\sigma=\sigma_{id}$). Assuming the stress-controlled quasistatic process, the solid system cannot reach its equilibrium state beyond these points since it disintegrates into isolated atoms in an unstable manner. This is, however, not the case of the total energy profiles in Fig. 1 since the equilibrium can be reached even beyond the inflection point when keeping the constant values of the crystal volume $V>V_{ip}$. Therefore, one can display quasistatic enthalpy curves beyond the instability point recalculated from the computed total energy curves for $V>V_{ip}$. Such a curve for the ground state of iron is plotted as a dashed line in Fig. 4. As expected, it lies above the solid line. For all computed systems, the dashed enthalpy curves must meet a point corresponding to the disintegrated configuration of free atoms, i.e., to the point $H_{(\sigma=0)}=U$, where U is the cohesive energy.

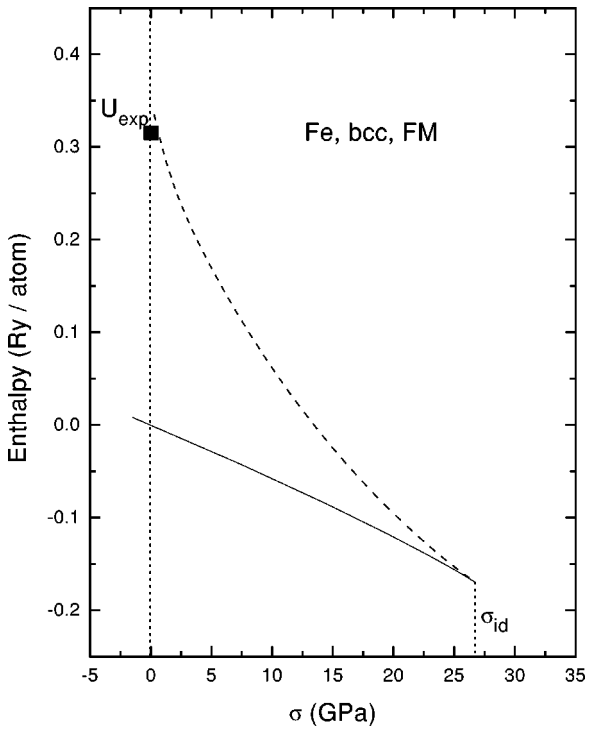

FIG. 4. Enthalpy of iron in the ground-state structure as a function of stress. The curves in the reversible (corresponding to $V<V_{ip}$) and the irreversible ($V>V_{ip}$) area are displayed by solid and dashed lines, respectively. The solid square displays the experimental value U_{expt} of cohesive energy.

The experimental value of U(Fe) is displayed as a solid square in Fig. 4. The usefulness of such enthalpy plots can be seen in a very clear and precise graphical determination of σ_{max} values corresponding to the intersection points of the solid and dashed curves.

As can be seen from Table II, the rough estimation $\sigma_{id}\approx B/7$ previously found on the basis of semiempirical methods[3,38] (assuming $\sigma_{id}=\sigma_{max}$) seems to be verified also by the *ab initio* approach. The computed values a_{ip}/a_0 related to the ideal strength σ_{id} amount all to about 15% similarly to other crystals.[5] This value is typically obtained from semiempirical calculations[38] as well.

It should be noted that the present discussion of the mechanical stability assessment is simplified since only a few competing structures were taken into account. Consequently, one cannot be completely sure that the ground-state structure remains stable before reaching the point of inflection. In order to asses the mechanical stability in a more reliable way, all stability conditions[39] and phonon spectra are to be analyzed.

For a cubic system under isotropic loading, three stability conditions have to be analyzed.[40,41] The first one is related to the point of inflection of the $E_{tot}(V)$ curve. The other two stability conditions include either the trigonal shear modulus C_{44} or the tetragonal shear modulus $C'=\frac{1}{2}(C_{11}-C_{12})$. Computing the shear moduli requires deformations lowering the symmetry of a crystal. Unfortunately, methods using the ASA are not convenient for such calculations, due to both the geometry violation and the error in the calculation of the

electrostatic term. Therefore, the full-potential treatment is necessary.[23,24] Our calculations testing these stability conditions are in progress. The currently obtained results for iron[42] really indicate that the instability associated with reaching the inflection point during isotropic tension appears as the first one. Similar results were obtained also for gold,[43] for alkali metals,[41] and for silicon and silicon carbide.[44] On the other hand, all the above-mentioned papers report the first appearance of shear types of instability in the compressive region. The same behavior was found in iron[18,45] and also reported in a recent study of the bcc-hcp transformation under pressure by Zhao *et al.*[46]

IV. CONCLUSION

In this paper we investigated the behavior of Fe, Co, Ni, and Cr at triaxial tension by means of the LMTO-ASA method. The ground-state structures of all investigated metals were correctly predicted when using the GGA together with the appropriate spin polarization. The best reproduction of experimental elastic and magnetic characteristics is mostly achieved by this approach as well. The total energy of the ground-state structures of all investigated metals remains the lowest one during the whole isotropic tensile deformation path up to the point of inflection. Similarly, the ground-state structure enthalpy is the lowest one for all isotropic tensile stresses up to σ_{max}. This fact suggests that the maximum stress at the inflection point on the dependence of total energy versus volume might be identified with the ideal strength under isotropic tension. Some recent and current studies of stability conditions also support this opinion (at least for iron). Except for Cr, the magnetic moments reach the zero value at a volume equal to about one-half of the equilibrium one.

ACKNOWLEDGMENTS

This research was supported by the Ministry of Education of the Czech Republic (Project No. CZ311002), by the Grant Agency of the Academy of Sciences of the Czech Republic (Project No. A1010817), by the Grant Agency of the Czech Republic (Project No. 106/02/0877), and by Research Project No. Z2041904 of the Academy of Sciences of the Czech Republic. A part of this study has been performed in the framework of COST Project No. OC 523.90. Use of the computer facility at the MetaCenter of the Masaryk University, Brno, and at the Brno University of Technology is acknowledged. The authors are grateful to Dr. I. Turek for useful discussions.

*Electronic address: mojmir@ipm.cz

[1] A. Kelly and N. H. Macmillan, *Strong Solids* (Clarendon Press, Oxford, 1986).
[2] J. Pokluda and P. Šandera, Phys. Status Solidi B **167**, 543 (1991).
[3] J. Pokluda and P. Šandera, Phys. Status Solidi B **160**, 89 (1990).
[4] P. Šandera, J. Pokluda, L. G. Wang, and M. Šob, Mater. Sci. Eng., A **234-236**, 370 (1997).
[5] M. Černý, P. Šandera, and J. Pokluda, Czech. J. Phys. **49**, 1495 (1999).
[6] Y. Song, R. Yang, and D. Li, Phys. Rev. B **59**, 14 220 (1999).
[7] D. J. Singh and J. Ashkenazi, Phys. Rev. B **46**, 11 570 (1992).
[8] B. I. Min, T. Oguchi, and A. J. Freeman, Phys. Rev. B **33**, 7852 (1986).
[9] T. C. Leung, C. T. Chan, and B. N. Harmon, Phys. Rev. B **44**, 2923 (1991).
[10] J. H. Cho and M. H. Kang, Phys. Rev. B **52**, 9159 (1995).
[11] Y. Shibutani, G. L. Krasko, M. Šob, and S. Yip, Mat. Sci. Res. Int. **5**, 225 (1999).
[12] D. J. Singh, W. E. Pickett, and H. Krakauer, Phys. Rev. B **43**, 11 628 (1991).
[13] M. Šob, M. Friák, L. G. Wang, and V. Vitek, in *Multiscale Modeling of Materials*, edited by V. V. Bulatov, T. Diaz de Rubia, R. Phillips, E. Kaxiras, and N. Ghoniem (Materials Research Society, Pittsburg, 1999), Vol. 538, p. 523.
[14] A. Y. Liu and D. J. Singh, Phys. Rev. B **47**, 8515 (1993).
[15] M. Friák, M. Šob, and V. Vitek, in *Proceedings of the International Conference JUNIORMAT'01*, edited by J. Švejcar (Faculty of Mechanical Engineering, Brno University of Technology, Brno, 2001), p. 117.
[16] D. M. Clatterbuck, D. C. Chrzan, and J. J. W. Morris, Philos. Mag. Lett. **82**, 141 (2002).
[17] M. Friák, M. Šob, and V. Vitek, Phys. Rev. B **63**, 052405 (2001).
[18] P. Söderlind, J. A. Moriarty, and J. M. Wills, Phys. Rev. B **53**, 14 063 (1996).
[19] G. L. Krasko and G. B. Olson, Phys. Rev. B **40**, 11 536 (1989).
[20] O. K. Andersen, Phys. Rev. B **12**, 3060 (1975).
[21] G. Krier, O. Jepsen, A. Burkhardt, and O. K. Andersen, TB-LMTO-ASA program, version 4.6, Max-Planck-Institut fur Festkörperforschung, Stuttgart, 1994.
[22] O. K. Andersen, O. Jepsen, and M. Šob, in *Electronic Band Structure and Its Applications*, edited by M. Yussouff (Springer-Verlag, Berlin, 1987), Vol. 40, p. 1.
[23] O. K. Andersen, M. Methfessel, C. O. Rodriguez, P. Blöchl, and H. M. Polatoglou, in *Atomistic Simulation of Materials—Beyond Pair Potentials*, edited by V. Vitek and D. Srolovitz (Plenum Press, New York, 1989), p. 1.
[24] M. Šob, L. G. Wang, and V. Vitek, Comput. Mater. Sci. **8**, 100 (1997).
[25] U. von Barth and L. Hedin, J. Phys. C **5**, 1629 (1972).
[26] J. P. Perdew and Y. Wang, Phys. Rev. B **45**, 13 244 (1992).
[27] V. L. Moruzzi and P. M. Marcus, Phys. Rev. B **42**, 8361 (1990).
[28] V. L. Moruzzi and P. M. Marcus, Phys. Rev. B **42**, 10 322 (1990).
[29] J. H. Cho and M. Scheffler, Phys. Rev. B **53**, 10 685 (1996).
[30] V. L. Moruzzi, J. F. Janak, and A. R. Williams, *Calculated Electronic Properties of Metals* (Pergamon Press, New York, 1978).
[31] C. Kittel, *Introduction to Solid State Physics* (Wiley, New York, 1976).
[32] G. Y. Guo and H. H. Wang, Phys. Rev. B **62**, 5136 (2000).
[33] E. G. Moroni, G. Kresse, J. Hafner, and J. Furthmüller, Phys. Rev. B **56**, 15 629 (1997).
[34] D. Bagayoko and J. Callaway, Phys. Rev. B **28**, 5419 (1983).
[35] *Handbook of Chemistry and Physics*, edited by D. R. Lide (CRC Press, Boca Raton, 1995).

[36] P. Bagno, O. Jepsen, and O. Gunnarsson, Phys. Rev. B **40**, 1997 (1989).
[37] M. Ekman, B. Sadigh, and K. Einarsdotter, Phys. Rev. B **58**, 5296 (1998).
[38] P. Šandera and J. Pokluda, Metall. Mater. Trans. A **32**, 180 (1994).
[39] *Thermodynamics of Crystals*, edited by D. C. Wallace (Wiley, New York, 1972).
[40] R. Hill and F. Milstein, Phys. Rev. B **15**, 3087 (1977).
[41] F. Milstein and D. J. Rasky, Phys. Rev. B **54**, 7016 (1996).
[42] M. Černý, M. Friák, M. Šob, J. Pokluda, and P. Šandera (unpublished).
[43] J. Wang, J. Li, S. Yip, S. Phillpot, and D. Wolf, Phys. Rev. B **52**, 12 627 (1995).
[44] S. Yip, J. Li, M. Tang, and J. Wang, Mater. Sci. Eng., A **317**, 236 (2001).
[45] H. Ma, S. Qiu, and P. Marcus, Phys. Rev. B **66**, 024113 (2002).
[46] J. Zhao, D. Maroudas, and F. Milstein, Phys. Rev. B **62**, 13 799 (2000).